ASF1 Binds to a Heterodimer of Histones H3 and H4: A Two-Step Mechanism for the Assembly of the H3−H4 Heterotetramer on DNA†

Christine M. English,‡ Nasib K. Maluf,§ Brian Tripet,‡ Mair E. A. Churchill,|| and Jessica K. Tyler*,‡

Department of Biochemistry and Molecular Genetics, University of Colorado Health Sciences Center at Fitzsimons, Aurora, Colorado 80045, Department of Pharmaceutical Sciences, University of Colorado Health Sciences Center, 4200 East Ninth Avenue, Denver, Colorado 80262, and Department of Pharmacology, University of Colorado Health Sciences Center at Fitzsimons, Aurora, Colorado 80045

Received July 11, 2005; Revised Manuscript Received August 30, 2005

ABSTRACT: The first step in the formation of the nucleosome is commonly assumed to be the deposition of a histone H3−H4 heterotetramer onto DNA. Antisilencing function 1 (ASF1) is a major histone H3−H4 chaperone that deposits histones H3 and H4 onto DNA. With a goal of understanding the mechanism of deposition of histones H3 and H4 onto DNA, we have determined the stoichiometry of the Asf1−H3−H4 complex. We have established that a single molecule of Asf1 binds to an H3−H4 heterodimer using gel filtration, amino acid, reversed-phase chromatography, and analytical ultracentrifugation analyses. We demonstrate that Asf1 blocks formation of the H3−H4 heterotetramer by a mechanism that likely involves occlusion of the H3−H3 dimerization interface.

In the eukaryotic nucleus, genomic DNA is assembled into the nucleoprotein complex known as chromatin. The basic repeating unit of chromatin is the nucleosome core particle, which consists of 146 bp of DNA wrapped around an octamer of histone proteins (*1*, *2*). The histone octamer comprises a tetramer of histones H3 and H4 and two dimers of H2A and H2B (*3*, *4*). Nucleosome core particles are regularly spaced every 180−200 bp of DNA over the entire genome, and the incorporation of the linker histones results in higher-order folding of these arrays of nucleosomes.

Every time the genome replicates the chromatin structure must also be duplicated. We know that the mechanism of chromatin assembly involves disassembly of the histone octamers from the parental chromatin into H3−H4 tetramers and H2A−H2B dimers, which are then distributed equally between the two new daughter DNA strands (*5*, *6*). The two daughter strands of chromatin are completed with newly synthesized histone H3−H4 tetramers and H2A−H2B dimers, which randomly mix with the parental H3−H4 tetramers and H2A−H2B dimers on the DNA (*7*). We also know that chromatin assembly occurs in a stepwise manner. Consistent with the central position that the H3−H4 tetramer occupies in the nucleosome, the H3−H4 tetramer is detected on the DNA first (*7*). H2A−H2B dimers, which bind at the periphery of the nucleosome, are deposited in the next step, followed by linker histone H1.

Chromatin assembly is mediated by chromatin assembly factors (*8*). The formation of the H3−H4 tetramer on DNA following replication is mediated by chromatin assembly factor 1 (CAF-1) in vitro (*9*), in a manner that is dependent on another H3−H4 chaperone termed antisilencing function 1 (Asf1) (*10*). It has recently been shown that the majority of non-chromatin-bound histones are bound to Asf1 prior to their assembly into chromatin, indicating that Asf1 is a central player in the process of chromatin assembly (*11*). Asf1 was first identified genetically as a suppressor of silencing when overexpressed in yeast (*12*, *13*), and was later identified biochemically as a component of the chromatin assembly factor RCAF (*10*). RCAF is a trisubunit complex comprised of Asf1 bound to newly synthesized histones H3 and H4. As a histone H3−H4 chaperone, Asf1 binds to the C-terminal portion of histone H3 between amino acid residues 122 and 135 (*14*). Asf1 has been highly conserved through evolution (*10*, *12*, *15*) with the exception of its C-terminal tail, which does not appear to be functionally important (*16*, *17*).

In addition to its biochemical function as a chromatin assembly factor, there is a wealth of in vivo evidence to indicate that Asf1 influences chromatin structure in the cell. Budding yeast lacking *ASF1* have altered global chromatin structure (*18*) and have defects in the processes that utilize the DNA template, including transcription (*19*−*22*), transcriptional silencing (*10*, *23*−*25*), and replication and repair (*10*, *26*−*28*). Although *ASF1* is essential in *Schizosaccharomyces pombe* and *Drosophila* (*16*, *29*), flies with a single copy of the *ASF1* gene show enhanced position effect variegation, which is a measure of altered chromatin structure (*29*). Asf1 also appears to be important for DNA replication in human cells, as tissue culture cells lacking Asf1 spend

† This work was supported by a grant from the National Institutes of Health (GM64475) to J.K.T. J.K.T. is a Leukemia & Lymphoma Society Scholar.

* To whom correspondence should be addressed: Department of Biochemistry and Molecular Genetics, University of Colorado Health Sciences Center at Fitzsimons, Mail Stop 8101, P.O. Box 6511, Aurora, CO 80045. Telephone: (303) 724-3224. Fax: (303) 724-3221. E-mail: Jessica.tyler@uchsc.edu.

‡ Department of Biochemistry and Molecular Genetics, University of Colorado Health Sciences Center at Fitzsimons.

§ University of Colorado Health Sciences Center.

|| Department of Pharmacology, University of Colorado Health Sciences Center at Fitzsimons.

10.1021/bi051333h CCC: $30.25
Published on Web 09/29/2005

more time in the S-phase (*11*). In addition to its role during the assembly of the H3−H4 tetramer into chromatin, Asf1 is also required for the disassembly of the H3−H4 tetramer from chromatin (*18*, *21*).

Until recently, the majority of data suggested that the non-chromatin-bound histones may exist as H3−H4 hetero-tetramers in the cell (*30*). Accordingly, it has been predicted that histones H3 and H4 are deposited onto DNA as an H3−H4 tetramer. However, a recent study has shown that endogenous histone H3 fails to copurify with epitope-tagged histone H3, suggesting that histones form an H3−H4 heterodimer rather than an H3−H4 heterotetramer in the cell (*31*). In the study presented here, we have investigated the stoichiometry of the Asf1−H3−H4 complex and found that Asf1 exists in a complex only with a heterodimer of histones H3 and H4. This work indicates that a novel step in nucleosome assembly and disassembly, the formation of the H3−H4 heterotetramer from the H3−H4 heterodimer and vice versa, needs to be considered in the study of processes that involve chromatin assembly and disassembly.

MATERIALS AND METHODS

Protein Expression and Purification. Plasmid pGST-Asf1tr was generated by insertion of the sequence encoding amino acids 1−169 of Asf1 from *Saccharomyces cerevisiae* into the EcoRI and XhoI restriction sites following the glutathione *S*-transferase cassette and PreScission protease sequence in the pGEX-6P-3 vector (Amersham Biosciences), using standard procedures. The fragment carrying the GST−Asf1tr fusion protein was PCR amplified from pGex-6P-3 using primers to introduce flanking EcoRI and XhoI restriction sites. This fragment was subcloned into a TopoTA (Invitrogen) vector and subsequently released using EcoRI and XhoI digestion and then subcloned into plasmid pET3aTr to generate plasmid pET3aTr-Asf1tr (*32*). The DNA sequence encoding amino acids 27−135 of *Xenopus laevis* histone H3 was inserted into the EcoRI and KpnI site of plasmid pET3aTr to generate plasmid pET3aTrH3ΔN. The DNA sequence encoding amino acids 20−102 of *X. laevis* histone H4 was inserted into the XbaI and BamHI site of plasmid pET3aTr to generate plasmid pET3aTrH4ΔN. The BspEI−MluI fragment of pET3aTr-Asf1tr carrying the ribosome binding site and the codons encoding the GST−Asf1tr fusion protein was inserted into the BspEI and MluI sites of plasmid pST39 to generate plasmid pST39GSTAsf1 (*32*). The EcoRI−KpnI fragment of pET3aTrH3ΔN, carrying the ribosome binding site and the N-terminally truncated H3, was inserted into the EcoRI and KpnI sites of plasmid pST39GSTAsf1 to generate plasmid pST39GSTAsf1H3. The XbaI−BamHI fragment of pET3aTrH4ΔN, carrying the ribosome binding site and the N-terminally truncated H4, was inserted into the XbaI and BamHI sites of plasmid pST39GSTAsf1H3 to generate plasmid pST39GSTAsf1H3H4. Coexpression of the GST−Asf1tr fusion protein, H3, and H4 was induced by addition of 0.4 mM IPTG to exponentially growing *Escherichia coli* Rosetta (pLys S) cells (Novagen) containing pST39GSTAsf1H3H4 for 8 h at 27 °C. Cell pellets from 1 L of cells were resuspended in 50 mL of buffer 1 [20 mM Tris-HCl (pH 7.9), 10 mM EDTA, 0.5 M NaCl, 1 mM PMSF, 0.7 μg/mL pepstatin, 0.5 μg/mL leupeptin, 2 μg/mL aprotonin, and 2 mM benzamidine] and lysed by sonication. The extract was clarified by centrifugation, and the soluble protein was incubated with 2 mL of a 50:50 glutathione−Sepharose (Amersham Biosciences) slurry for 2 h at 4 °C. The resin was washed 10 times with 1 mL of buffer 2 [20 mM Tris-HCl (pH 7.9), 10 mM EDTA, 1 M NaCl, 1 mM PMSF, 0.7 μg/mL pepstatin, 0.5 μg/mL leupeptin, 2 μg/mL aprotonin, and 2 mM benzamidine] and five times with 1 mL of PreScission cleavage buffer [50 mM Tris-HCl (pH 7.0), 150 mM NaCl, 1 mM EDTA, 1 mM DTT, 0.7 μg/mL pepstatin, 0.5 μg/mL leupeptin, and 2 μg/mL aprotonin]. The GST tag was then cleaved from the GST−Asf1tr fusion protein using PreScission protease (Amersham Biosciences) for 16 h at 4 °C, to release the Asf1tr−H3−H4 complex.

Gel Filtration Chromatography of the Asf1tr−H3−H4 Complex. A HiLoad 16/60 Superdex 75 prep grade gel filtration column (Amersham Biosciences) was equilibrated in running buffer [10 mM Tris-HCl (pH 7.9) and 0.5 M NaCl] at a flow rate of 1 mL/min. A calibration curve was prepared by running blue dextran (2000 kDa), bovine serum albumin (67 kDa), ovalbumin (43 kDa), carbonic anhydrase (29 kDa), and cytochrome *c* (12 kDa) (Amersham Biosciences) on the column. The elution of these markers was monitored by UV absorption at 280 nm, and the elution volume for each protein was measured from the start of the sample application to the apex of the elution peak. The logarithm of molecular weight was plotted against K_{av} that was calculated for each protein with the equation $K_{av} = V_e - V_o/V_t - V_o$, where V_e is the elution volume for the protein, V_o is the column void volume, which equals the elution volume of blue dextran 2000, and V_t is the total column volume. The cleaved Asf1tr−H3−H4 complex was concentrated to a volume of 2 mL using 5000 molecular weight cutoff (MWCO) Amicon Ultra-15 centrifugal filter devices (Millipore) before being loaded onto the column. Fractions were analyzed by SDS−PAGE and stained with Coomassie blue. Fractions from peaks containing either the Asf1tr−H3−H4 complex or the Asf1tr protein alone were pooled for further experiments.

Plasmid Supercoiling Assay. The Asf1tr−H3−H4 complex was tested for its ability to promote supercoiling onto relaxed plasmid DNA, as a measure of chromatin assembly activity, as previously described (*10*). Briefly, all reaction mixtures contained 20 μL of cytosolic extract derived from human 293 cells, ATP, an ATP regenerating system, and 100 ng of plasmid pCRK. The Asf1tr−H3−H4 complex from the gel filtration column was added, as indicated in Figure 2. As a positive control, 1 μL of *Drosophila* embryo S190 extract was used. For comparison, Asf1tr from the gel filtration analysis was also tested. Reaction mixtures were incubated for 90 min at 30 °C, after which time the reactions were stopped with EDTA. Following deproteinization, DNA samples were analyzed on a 1% agarose gel and stained with Syber Gold (Molecular Probes).

Amino Acid Analysis. The amino acid composition of the Asf1tr−H3−H4 complex was determined by hydrolyzing the purified complex in 6 N HCl containing 0.1% phenol for 24 h at 110 °C in evacuated, sealed tubes. Following the removal of HCl by vacuum, samples were dissolved in sample dilution buffer (0.2 M sodium citrate/HCl, 0.5% thiodiglycol, 0.1% benzoic acid, pH 2 buffer) and analyzed on a Beckman model 6300 amino acid analyzer (Beckman Instruments, Berkeley, CA).

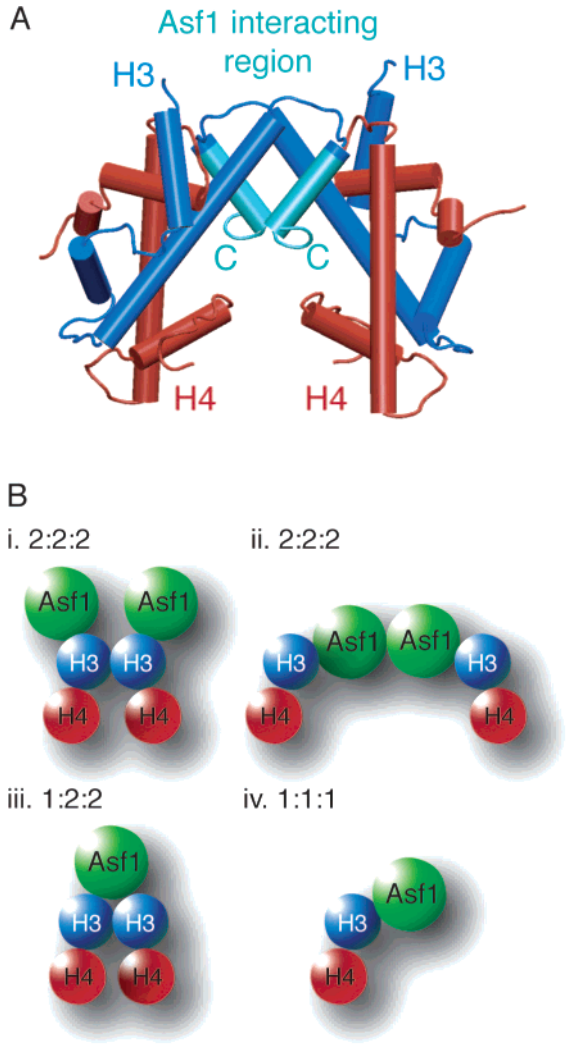

FIGURE 1: Model for histone binding by Asf1. (A) Cartoon diagram of the H3−H4 heterotetramer. Blue depicts the H3 dimer; red depicts two H4 molecules, and cyan depicts the putative Asf1−H3 interacting region at the H3−H3 dimerization interface (amino acids 97−135). The model was derived from the coordinates of the nucleosome structure of PDB entry ikx5 (*37*). (B) Schematic of possible models for interaction among Asf1, H3, and H4. (i) Model for a 2:2:2 stoichiometric Asf1:H3:H4 ratio, where two Asf1 molecules would bind to the identical interaction surfaces on each of the H3 proteins within the H3−H4 heterotetramer. (ii) Model for a 2:2:2 stoichiometric Asf1:H3:H4 ratio, where interaction between Asf1 and two H3−H4 heterodimers is mediated via a hypothetical Asf1−Asf1 interaction. (iii) Model for a 1:2:2 stoichiometric Asf1:H3:H4 ratio, where interaction between Asf1 and the H3−H4 tetramer is mediated via binding of Asf1 to H3. This model would require that each Asf1 molecule have two identical binding interfaces for H3. (iv) Model for a 1:1:1 stoichiometric Asf1:H3:H4 ratio, where interaction between Asf1 and the H3−H4 heterodimer is mediated via binding of Asf1 to the H3 dimerization interface.

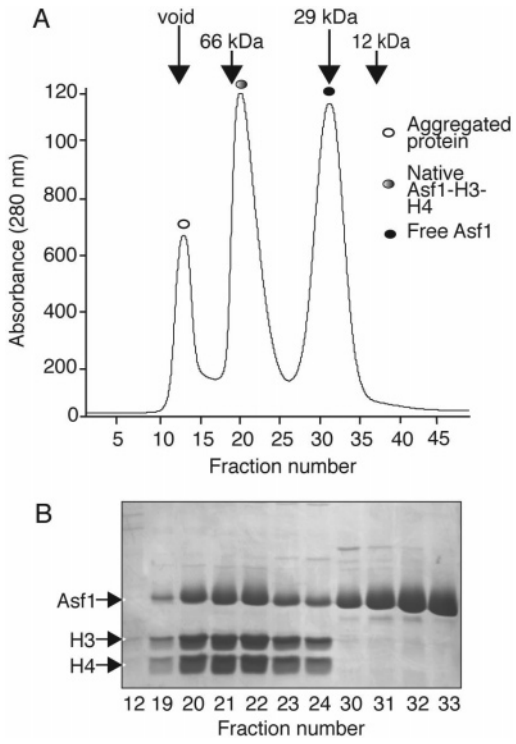

FIGURE 2: Gel filtration analysis of the recombinant Asf1−H3−H4 complex. (A) Elution profile of the Asf−H3−H4 complex obtained by gel filtration analysis. Recombinant Asf1tr−H3−H4 complex was eluted from a Superdex 75 16/60 HiLoad column, and the resulting trace is shown. The key indicates the identity of the major peaks, as determined by SDS−PAGE analysis of selected fractions. The arrows indicate the positions of the elution peaks of gel filtration standards that were eluted from the same column in the same buffer as the Asf1tr−H3−H4 complex. (B) SDS−PAGE analysis of the purified Asf1tr−H3−H4 complex obtained by gel filtration analysis. Selected fractions from the gel filtration column elution profile shown in panel A were resolved on a 15% polyacrylamide gel and stained with Coomassie blue. The positions of the Asf1, H3, and H4 proteins are indicated.

Reversed-Phase Chromatography. The purified Asf1tr−H3−H4 complex (5 mg/mL) was diluted 1:1 with a solution of 6 M GdnHCl and incubated for 30 min at room temperature. The denatured mixture was then applied to an analytical C8 reversed-phase column [Zobax 300SB-C8, 15 cm × 4.6 mm (inner diameter), 5 μm particle size, 300 Å pore size; Agilent Technologies]. The proteins were eluted from the column using a linear gradient of A and B, where eluent A was 0.05% aqueous trifluoroacetic acid and eluant B was 0.05% trifluoroacetic acid in acetonitrile at a flow rate of 1.0 mL/min at room temperature. A sample of each eluting peak was taken to establish the identity of each subunit using a Mariner ESI-TOF mass spectrometer (Applied Biosystems, Foster City, CA). To calculate the protein ratio in the Asf1tr−H3−H4 complex relative to the H4 protein, each peak area was divided by the peak area for the H4 protein.

Sedimentation Velocity Experiments. Sedimentation velocity experiments were performed using a Beckman XLA analytical ultracentrifuge (Beckman Instruments, Inc., Fullerton, CA) equipped with absorbance optics and an An60Ti rotor. The Asf1tr−H3−H4 complex that eluted from the gel filtration column was loaded into Epon charcoal-filled two-sector centerpieces, and running buffer [10 mM Tris (pH 7.9), 0.5 M NaCl, and 1 mM TCEP] was used for the reference chamber. Experiments were performed at 42 000 rpm and 4 °C. Data were collected at a wavelength of 280 nm, using a spacing of 0.005 cm, with four averages in the continuous scan mode. No time delay was used, allowing traces to be collected every 3−6 min, depending upon the number of cells used in a run. Sedimentation coefficients were corrected to standard conditions (20 °C, in water) using SEDNTERP (D. Hayes, Magdalen College, Oxford, U.K.; T. Laue, University of New Hampshire, Durham, NH; J. Philo, Amgen, Thousand Oaks, CA). The sedimentation

velocity data were analyzed using the time-derivative method, according to Stafford (*33*), using the DCDT+ software (*34*), to obtain the $g(s^*)$ distribution of the sample. The $g(s^*)$ distributions were further analyzed according to the method of Stafford (*35*), to obtain the apparent molecular weight of the sample; this analysis is possible if the sample is composed of a homogeneous species. The $g(s^*)$ distributions were fitted to a single Gaussian distribution, according to eq 1:

$$g(s^*) = \frac{A}{\sigma\sqrt{2\pi}} \exp\left[-\frac{(s^*_{20,w} - s_{20,w})^2}{2\sigma^2}\right] + b \qquad (1)$$

where A is the total absorbance of the sample at the plateau, $s^*_{20,w}$ is the apparent sedimentation coefficient (corrected to standard conditions), $s^*_{20,w}$ is the sedimentation coefficient (corrected to standard conditions) of the complex, and corresponds to the peak value of the $g(s^*)$ distribution, b is the baseline offset, and σ is the width parameter. σ is related to the diffusion coefficient of the protein complex according to eq 2 (*35*):

$$D_{20,w} = 0.5\sigma^2 r_m{}^2 \omega^2 \int_{t=0}^{t} \omega^2 \, dt \qquad (2)$$

where $D_{20,w}$ is the diffusion coefficient of the macromolecule, r_m is the radial position of the sample meniscus, ω is the rotor speed, and t is the sedimentation time. The corresponding values for $s_{20,w}$ and $D_{20,w}$ were then used to calculate the molecular weight of the macromolecule (*35*), according to the Svedberg equation (rearranged to solve for M):

$$M = \frac{s_{20,w} RT}{D_{20,w}(1 - \bar{v}\rho)} \qquad (3)$$

where M is the molecular weight of the macromolecule, R is the gas constant, T is the absolute temperature, $\bar{v}$ is the partial specific volume of the Asf1−H3−H4 complex, and ρ is the buffer density. ρ was calculated using SEDNTERP. $\bar{v}$ (for the complex) was calculated from the amino acid composition of Asf1, H3, and H4, assuming a 1:1:1 ratio, according to the method of Cohn and Edsall (*36*) using SEDNTERP, which gave 0.7247 mL/g at 4 °C. The calculated molecular weight of the complex is 41 879.

The van Holde−Weischet analysis of the sedimentation velocity data was performed using Borris Demler's program Ultrascan (http://www.ultrascan.edu).

Sedimentation Equilibrium Experiments. The Asf1tr−H3−H4 complex that eluted from the gel filtration column was diluted with the running buffer (the identical buffer used for the sedimentation velocity experiments), and loaded into each of three sample chambers (120 μL per chamber) in an Epon charcoal-filled six-channel centerpiece, and the running buffer was used for the reference chambers. Three loading concentrations of the complex were analyzed: 0.35, 0.2, and 0.1 mg/mL. The complex was successively sedimented to equilibrium at three rotor speeds: 20K, 25K, and 30K rpm at 4 °C. Equilibrium was established within 24 h for each speed. This was checked by comparing at least three successive scans, each taken 2 h apart, to determine if the scans overlayed each other. Scans were collected at 280 nm, every 0.001 cm, with 15 averages per step. The absorbance traces were edited using REEDIT (J. Lary, National Analytical Ultracentrifuge Center, Storrs, CT) to extract the data between the sample meniscus and the bottom of the sample cell. The sedimentation equilibrium data were analyzed using the nonlinear least-squares program WINNONLIN (D. Yphantis, University of Connecticut, Storrs, CT; M. Johnson, University of Virginia, Chrlottesville, VA; J. Lary, National Analytical Ultracentrifuge Center). The data were fit globally (each protein loading concentration at each rotor speed, for a total of nine data sets) to an ideal, single-species model, shown in eq 4:

$$A_T = \exp(\ln A + \sigma\xi) + b \qquad (4)$$

where A_T is the total absorbance as a function of radial position, A is the absorbance of the protein complex at a reference radial position, r_{ref} (taken as the radial position of the first data point), b is the baseline offset, and $\xi = 0.5(r^2 - r_{ref}{}^2)$. σ is the reduced molecular weight of the protein complex, and is given by

$$\sigma = \frac{M(1 - \bar{v}\rho)\omega^2}{RT} \qquad (5)$$

RESULTS

Rationale for Analysis of Stoichiometry of the Asf1−H3−H4 Complex. To gain insight into the mechanism of Asf1-mediated chromatin assembly, we chose to determine the stoichiometry of Asf1 bound to histones H3 and H4. The general assumption in the field is that free histones H3 and H4 exist as a heterotetramer in the cell and are deposited as a heterotetramer onto DNA by histone chaperones. Interestingly, the region of histone H3 that mediates the H3−H3 interaction, which is an important protein interaction region within the H3−H4 heterotetramer, is the same region that binds to Asf1 (Figure 1A) (*14*, *15*). The idea that Asf1 may bind to an H3−H4 heterodimer, and in doing so may block the interaction between the two H3−H4 heterodimers, would indicate that assembly of the H3−H4 heterotetramer onto the DNA is a two-step mechanism requiring the deposition of two H3−H4 heterodimers. As such, it was important to determine unequivocally whether Asf1 binds to an H3−H4 heterodimer, an H3−H4 heterotetramer, or both. Several models showing the potential stoichiometry for the Asf1−H3−H4 complex that are tested in this work are shown in Figure 1B.

Generation of a Complex of Asf1 Bound to Histones H3 and H4. To determine whether Asf1 binds to a heterodimer or a heterotetramer of histones H3 and H4, we set out to obtain large quantities of the purified Asf1−H3−H4 complex for biophysical analysis. It was not possible to purify sufficient quantities of the native Asf1−H3−H4 complex (also called RCAF) from *Drosophila* embryos for our purposes (*10*); therefore, we generated recombinant Asf1−H3−H4 complex. To obtain recombinant Asf1−H3−H4 complex, we coexpressed the three open reading frames as a polycistronic message in *E. coli* (*32*). This was necessary to generate a soluble complex of Asf1 bound to histones H3 and H4 (Figure 2 and data not shown). We expressed the stable domain of yeast Asf1 (*17*), which we call "Asf1tr", as a GST fusion, together with the globular domains of the H3 and H4 proteins (*37*). Following cleavage from the glutathione−Sepharose resin, the protein complex was puri-

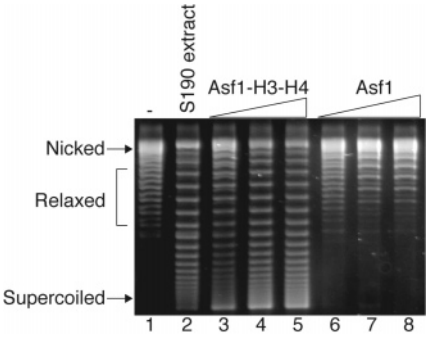

FIGURE 3: Recombinant Asftr−H3−H4 complex has nucleosome assembly activity. The ability of nothing (−), *Drosophila* S190 extract, increasing amounts of purified recombinant Asf1tr−H3−H4 complex (400 ng, 750 ng, or 1 μg), or recombinant Asf1 (400 ng, 750 ng, or 1 μg) to introduce supercoils into relaxed plasmid DNA in a DNA replication-independent supercoiling assay was tested. An image of a Sybr gold stained agarose gel is shown with markers for supercoiled and relaxed species as indicated.

fied by gel filtration chromatography (Figure 2A). The Asf1tr−H3−H4 complex, high-molecular weight plus aggregated proteins, and free Asf1tr eluted from a HiLoad 16/60 Superdex 75 column in three distinct peaks, as revealed by SDS−PAGE analysis (Figure 2B). The existence of a soluble Asf1tr−H3−H4 complex confirms that neither the nonconserved C-terminus of Asf1 nor the N-terminal tails of H4 and H3 are required for the interaction between Asf1 and histones. Furthermore, the fact that the interaction between the Asf1tr−H3−H4 complex is maintained at 0.5 M NaCl (Figure 2) indicates that this is a highly stable complex as this concentration of salt pushes the equilibrium toward tetramers (*38*).

The Asf1tr−H3−H4 Complex Is Competent To Assemble Nucleosomes. To demonstrate that the recombinant Asf1tr−H3−H4 complex is active and able to assemble nucleosomes, we examined the ability of the Asf1tr−H3−H4 complex to promote plasmid supercoiling. The assembly of each nucleosome onto a closed circle of DNA results in the incorporation of a supercoil into the plasmid (*39*). We had previously shown that RCAF (i.e., the endogenous Asf1−H3−H4 complex purified from *Drosophila* embryos) could assemble nonreplicating DNA into chromatin in the absence of chromatin assembly factor 1, as assessed by plasmid supercoiling (*10*). Therefore, we used this assay to test the assembly activity of the recombinant Asf1tr−H3−H4 complex. As a positive control for chromatin assembly, we included a *Drosophila* embryo S190 extract that is known to promote plasmid supercoiling in this assay (*10*) (Figure 3, lane 2). The purified Asf1tr−H3−H4 complex efficiently introduced supercoils onto relaxed plasmid DNA (Figure 3, lanes 3−5), indicating that it can mediate chromatin assembly. The human 293 cell extract present in the assay includes sufficient histones for chromatin assembly (*10*). Therefore, we asked whether the manner in which Asf1 presents the histones is important for chromatin assembly. To answer this question, we tested whether Asf1 alone was able to mediate the assembly of the histones from the 293 extract onto plasmid DNA. We found that purified Asf1tr failed to promote plasmid supercoiling (Figure 3, lanes 6−8). As such, free Asf1 cannot utilize the histones in the 293 extract during chromatin assembly. Furthermore, addition of histones alone does not result in supercoiling of the plasmid DNA in this assay (*10*). These results indicate that the Asf1tr−H3−H4 complex is functional for chromatin assembly and that the histones bound to Asf1tr are presented in a manner that allows their deposition onto DNA.

Gel Filtration Analysis of the Asf1tr−H3−H4 Complex. To determine the approximate size of the Asf1tr−H3−H4 complex, we examined its elution volume on gel filtration analysis. The K_{av} value of the elution peak of the Asf1tr−H3−H4 complex was calculated and interpolated on a calibration curve of known molecular weight standards analyzed on the same column, as described in Experimental Procedures (Figure 2). The molecular mass calculated for the Asf1tr−H3−H4 complex is 55 ± 4 kDa (expressed as the mean ± the standard deviation of three independent experiments). The predicted molecular mass of the Asf1tr−H3−H4 complex containing one molecule of each protein (1:1:1) is 42 kDa (19.7 kDa + 12.7 kDa + 9.6 kDa), while 1:2:2 and 2:2:2 complexes would have predicted molecular masses of 64 and 84 kDa, respectively. This result suggests that Asf1 may bind to the H3−H4 tetramer in either a 1:1:1 or 1:2:2 ratio but most likely not in a 2:2:2 ratio. In a similar manner, we calculated the size of the Asf1tr protein by gel filtration analysis as being 27.5 ± 1 kDa. The expected size of a monomer of Asf1tr is 19.7 kDa.

The Asf1tr−H3−H4 Complex Is Equimolar. The elution of proteins during gel filtration analysis is influenced by the shape of the protein, and as such is not an accurate measure of mass. To more accurately investigate the stoichiometry of the Asf1tr−H3−H4 complex, we examined the amino acid composition of the complex. We calculated the relative amount of the amino acids that are present in a theoretical 1:2:2 and 1:1:1 (or 2:2:2) Asf1tr−H3−H4 complex and compared those values to the actual number of amino acids observed for the Asf1tr−H3−H4 complex (Figure 4). Only amino acid residues that are statistically different between the 1:2:2 and 1:1:1 (or 2:2:2) ratio can be used for the analysis and are denoted with asterisks in Figure 4. Comparison of the observed ratio of these amino acids (normalized to alanine) for the Asf1tr−H3−H4 complex and the theoretical amino acid ratios for a 1:2:2 and 1:1:1 (or 2:2:2) Asf1tr−H3−H4 complex for these amino acids demonstrated that the observed values correlate most closely with the theoretical 1:1:1 (or 2:2:2) complex.

Next, we used reversed-phase chromatography to further analyze whether the stoichiometry of the Asf1tr−H3−H4 complex is 1:2:2 or equimolar (1:1:1 or 2:2:2). The purified Asf1tr−H3−H4 complex was applied to an analytical C8 reversed-phase column, and the eluted proteins were subjected to mass spectrometry analysis (Figure 5). The theoretical ratio of proteins calculated for a 1:1:1 (or 2:2:2) and 1:2:2 complex, based on molecular weight, was compared to the observed protein ratio for the Asf1tr−H3−H4 complex. To calculate the protein ratio in the Asf1tr−H3−H4 complex, the peak areas of each component were divided by the peak area of the H4 protein. The theoretical ratio for a 1:1:1 (or 2:2:2) Asf1tr−H3−H4 complex was calculated to be 2.1:1.3:1 and for a complex with a theoretical ratio of 1:2:2 would be 2.2:2.6:2. The observed integrated area units for the Asftr−H3−H4 complex were 2.3:1.3:1. Comparison of the theoretical 1:1:1 (or 2:2:2) complex with the observed integrated area units for the Asf1tr−H3−H4 complex demonstrates almost identical protein ratios. Taken together,

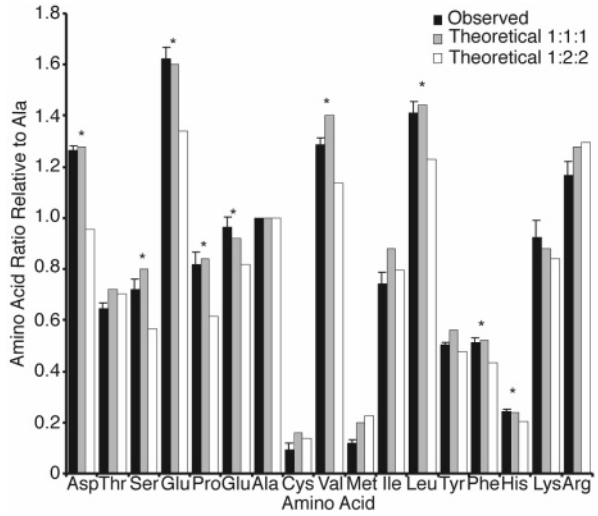

FIGURE 4: Amino acid analysis indicates equal stoichiometry in the Asf1tr−H3−H4 complex. The amino acid content of recombinant Asf1tr−H3−H4 complex from the gel filtration analysis shown in Figure 1 was determined. The observed ratio of each amino acid in the Asf1tr−H3−H4 complex, relative to alanine (normalized to 1), is represented by the black bars. The error bars indicate the standard deviation of three independent experiments. The expected ratio for a theoretical 1:1:1 Asf1tr−H3−H4 complex is shown with gray bars, while the expected ratio for a theoretical 1:2:2 Asf1tr−H3−H4 complex is shown with white bars. The asterisks indicate the amino acid residues that are significantly different between the 1:1:1 and 1:2:2 complex and can thus be used for determining the stoichiometry of the recombinant Asf1tr−H3−H4 complex.

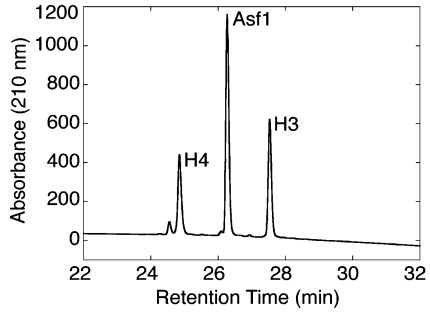

FIGURE 5: Reversed-phase HPLC analysis indicates the equal stoichiometry in the Asf1tr−H3−H4 complex. Purified recombinant Asf1tr−H3−H4 complex was analyzed by reversed-phase HPLC at 210 nm and normalized to H4, and the resulting elution profile is shown. The identity of the protein eluting in each peak was determined by mass spectrometry, and is indicated. The ratio of the integrated area units under each peak is 2.3:1.3:1 for the Asf1tr−H3−H4 complex.

the amino acid analysis and reversed-phase chromatography analysis indicate that the Asf1tr−H3−H4 complex contains equimolar amounts of each protein, and is consistent with either a 1:1:1 or 2:2:2 complex.

The Molecular Weight for the Asf1tr−H3−H4 Complex Is Consistent with a Heterotrimer. To unequivocally determine the stoichiometry of the Asf1tr−H3−H4 complex, we utilized analytical ultracentrifugation. Six samples over an approximate 10-fold concentration range of the Asf1tr−H3−H4 complex (from 0.074 to 0.64 mg/mL) were subjected to sedimentation velocity analysis. To assess the homogeneity of the sample, a van Holde−Weischet analysis was performed on the data. A representative analysis is shown in Figure 6A, for a protein concentration of 0.31 mg/mL. The vertical distribution of $s_{20,w}$ indicates the sample consists of

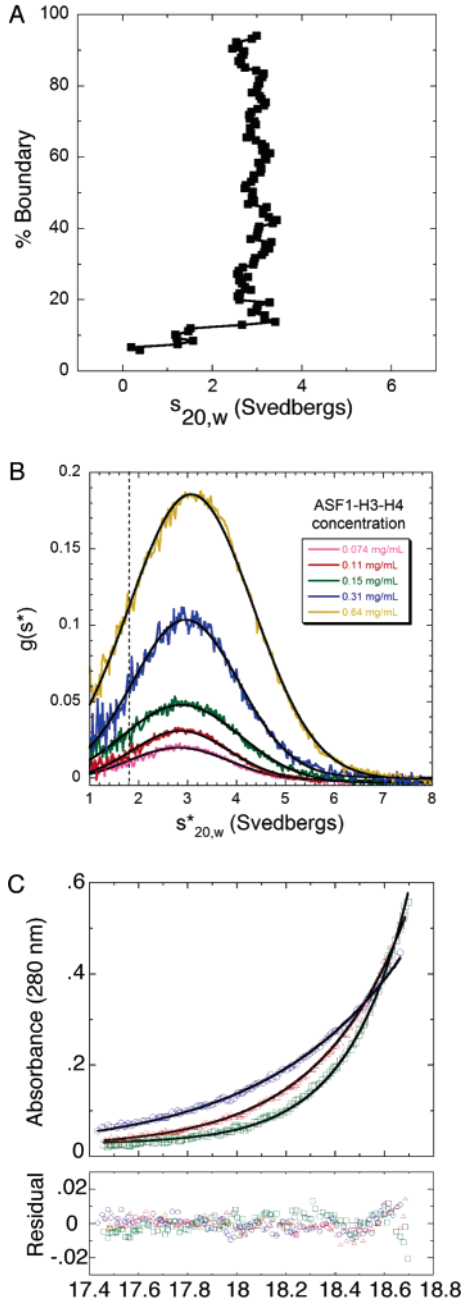

FIGURE 6: Analytical ultracentrifugation analyses demonstrate that the Asf1tr−H3−H4 complex exists as a single 2.9S species in solution. (A) Analysis of the homogeneity of the Asf1tr−H3−H4 sample. van Holde−Weischet analysis of sedimentation velocity analysis of 0.31 mg/mL Asf1tr−H3−H4 complex. Over the majority of the boundary, the sample is characterized by a single value of $s_{20,w}$ of ~3 S. (B) Sedimentation velocity analysis of the Asf1tr−H3−H4 complex. The calculated $g(s^*)$ distributions from the sedimentation velocity experiments are shown for increasing loading concentrations of the complex (from 0.074 to 0.64 mg/mL). The smooth curves are the nonlinear least-squares fits of the $g(s^*)$ data to a single Gaussian distribution (eq 1). The dotted line corresponds to the sedimentation value of Asf1 alone; $s_{20,w}$ is 1.93 ± 0.02 S, and the molecular mass is 18.7 ± 1.2 kDa. (C) Sedimentation equilibrium analysis of the Asf1tr−H3−H4 complex. The Asf1tr−H3−H4 complex (0.35 mg/mL) was sedimented to equilibrium at 20K (blue circles), 25K (red triangles), and 30K rpm (green squares), at 4 °C. The top panel shows the results of a global, nonlinear least-squares fit of the data to a single-ideal species model (the smooth curves that are drawn through the data). The bottom panel shows the residuals for this fit.

a single, homogeneous species (with $s_{20,w} \sim 3$ S), with no evidence for concentration-dependent self-association. Next, a $g(s^*)$ analysis was performed on the data, and the results are shown in Figure 6B. This analysis demonstrates that there is no shift in the peak position of the $g(s)$ curves with an increase in the concentration of the Asf1tr−H3−H4 complex as analyzed by DCDT+ (*34*). These data suggest a single, homogeneous species is present at all concentrations that were examined. If the sample is homogeneous, analysis of these curves allows for an estimation of the molecular weight of the complex (*35*). These curves were fit to Gaussian distributions to calculate the diffusion coefficient for the Asf1tr−H3−H4 complex. The diffusion coefficient, along with the average value for $s_{20,w}$ [the peak of the $g(s^*)$ distribution] of 2.92 ± 0.1S, allows for calculation of the molecular mass of the Asf1tr−H3−H4 complex as 37 ± 4 kDa. We also derived the same molecular mass when we fit the sedimentation velocity data to John Philo's program SVEDBERG (data not shown). Given that the theoretical calculated molecular mass of a 1:1:1 Asf1tr−H3−H4 complex is 42 kDa, these results indicate that a single molecule of Asf1tr binds to a heterodimer of histones H3 and H4.

To provide further evidence that Asf1tr binds to a heterodimer of histones H3 and H4, we utilized sedimentation equilibrium analysis. Sedimentation equilibrium studies were performed under identical conditions as sedimentation velocity and gel filtration analyses as described in Experimental Procedures. Three different concentrations of the Asf1tr−H3−H4 complex were analyzed by this technique: 0.1, 0.2, and 0.35 mg/mL. Data are presented only for 0.35 mg/mL because the data for all concentrations are identical (data not shown). The complex was sedimented to equilibrium at 20K, 25K, and 30K rpm at 4 °C, and the data were fit to different models. The data fit the single-species model very well (standard deviation of the fit was 4.2e-3 OD units, compared to a noise level in the optics of 3.5e-3 OD units) (Figure 6C). The value for the molecular mass of the complex obtained from fitting the data to the single-species model was 38.4 ± 3 kDa. We also derived the same molecular weight when we fit the sedimentation velocity data. Taken together, the analytical ultracentrifugation results demonstrate that the Asf1tr−H3−H4 complex has a molecular mass of 38.4 ± 3 kDa (based on equilibrium data) and 37 ± 4 kDa (based on velocity data) (Figure 6B,C). The data from these two experiments are in close agreement, which indicates that the complex purified from gel filtration is homogeneous and that the molecular masses derived from the analytical ultracentrifugation analysis are likely to be precise. The molecular masses of the complex obtained by analytical ultracentrifugation analysis are slightly smaller than the calculated molecular mass of 41.8 kDa for the 1:1:1 complex, but this can be attributed to not having a precise value for the partial specific volume of the molecule. Because these experiments were performed in 0.5 M NaCl, the actual partial specific volume is expected to increase slightly which will result in a slight underestimate of the true molecular weight (*40*). For example, data for oxyhemoglobin show that the apparent isopotential specific volume increases by 2.1% from 0 to 0.5 M NaCl (extrapolated using data in ref *41*). If the partial specific volume of the Asf1tr−H3−H4 complex increases by a similar amount, the calculated value for the molecular mass, based on the sedimentation equilibrium data, would increase to 40.9 ± 3 kDa, well within our experimental uncertainty.

The Asf1tr protein was also analyzed by analytical ultracentrifugation (Figure 6B). The sedimentation coefficient calculated for this protein was 1.93 ± 0.02 S, which corresponds to a molecular mass of 18.7 ± 1.2 kDa (data not shown), as compared to the predicted molecular mass of 19 kDa. This result indicates that Asf1 is homogeneous and exists as a monomer in solution, and is consistent with an Asf1 monomer binding to a heterodimer of H3 and H4.

DISCUSSION

It is widely considered that non-chromatin-bound histones H3 and H4 exist in the cell as a heterotetramer, and that they are deposited onto DNA as a heterotetramer (for recent reviews, see refs *42* and *43*). The basis of this assumption appears to be a combination of the following observations. (1) Extraction of histones from chromatin using conditions such as high salt or acid yields H3−H4 heterotetramers and H2A−H2B heterodimers (*44*). (2) The H3−H4 heterotetramer extracted from chromatin is highly stable in solution (*38*). (3) If highly purified histones are folded together in vitro, the end result is an H3−H4 tetramer (*3*, *45*, *46*). (4) Old H3−H4 histones and new H3−H4 histones do not intermix during replication, indicating that the H3−H4 tetramers remain intact once formed (*6*). (5) The first intermediate of chromatin assembly that has been detected is the H3−H4 heterotetramer bound to DNA (*47*).

We show for the first time, unequivocally, that the histone chaperone Asf1 binds to a heterodimer of histones H3 and H4. The physiological relevance of Asf1 binding to an H3−H4 heterodimer in vitro is supported by the size of the endogenous Asf1−H3−H4 complex. We previously found that the native Asf1−H3−H4 complex (RCAF) purified from *Drosophila* embryos has a native mass of around 66 kDa as determined by gel filtration analysis (*10*), which is between the calculated mass of 53 kDa for a 1:1:1 complex and 80 kDa for a 1:2:2 complex. Gel filtration analysis of our recombinant Asf1tr−H3−H4 complex also gave an apparent molecular mass that was between the calculated masses for the 1:1:1 and 1:2:2 complexes (Figure 2). However, our biophysical analyses proved that the recombinant Asf1tr−H3−H4 complex is in fact a 1:1:1 complex, indicating that the Asf1−H3−H4 complex elutes from gel filtration analysis with a larger apparent size than its actual size. As such, we can infer that native Asf1 is also bound to an H3−H4 heterodimer. Furthermore, the majority of non-chromatin-bound histone H3 in human cells is in a complex with Asf1 (*11*). Therefore, it is likely that the majority of non-chromatin-bound histones H3 and H4 are present as H3−H4 heterodimers and not H3−H4 heterotetramers in the cell. Consistent with this idea, a recent affinity purification analysis of epitope-tagged histone H3 demonstrated the absence of copurifying endogenous H3, suggesting that non-chromatin-bound histones H3 and H4 may exist as a heterodimer in vivo (*31*).

We have produced the recombinant Asf1−H3−H4 complex under entirely native conditions. It is important to contrast this to the typical behavior of recombinant histones, which are always expressed in inclusion bodies in *E. coli*

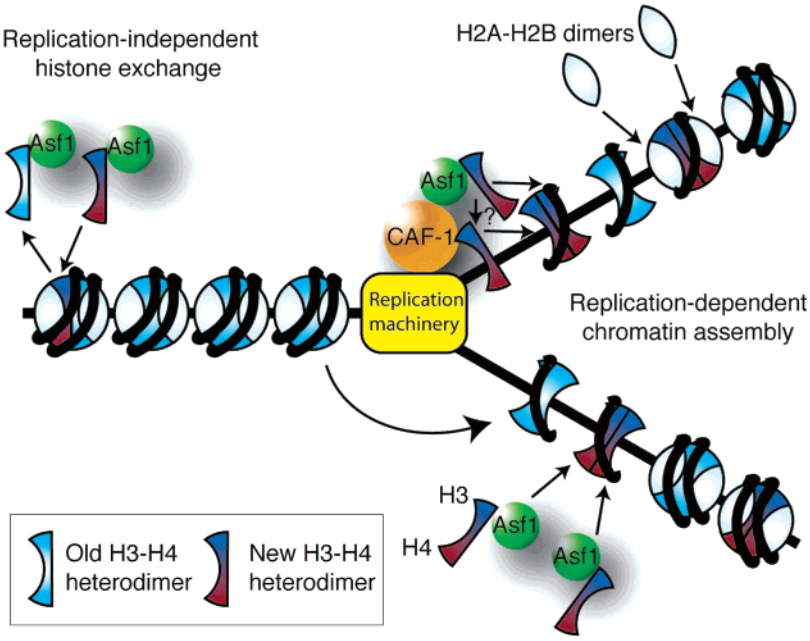

FIGURE 7: Model for stepwise formation of the H3−H4 heterotetamer on DNA. Old H3−H4 heterotetramers (light blue apple cores) are randomly distributed between the new daughter strands of DNA, while Asf1 and/or CAF-1 deposits new H3−H4 heterodimers onto the newly replicated DNA to form new H3−H4 heterotetramers (red and blue apple cores). Asf1 binds to the H3 dimerization interface of the H3−H4 heterodimer, preventing its dimerization to form an H3−H4 heterotetramer until Asf1 releases the histones. Asf1 may pass the H3−H4 heterodimers to its binding partner CAF-1 to be deposited onto the newly replicated DNA, or Asf1 may deposit the H3−H4 heterodimers directly. CAF-1 is localized to the replication fork via interaction with the replication machinery. Asf1 is also required for replication-independent chromatin disassembly and assembly, otherwise known as histone exchange, which results in the mixing of old and new heterodimers within an H3−H4 heterotetramer.

(*37*). Therefore, this study uses proteins that have always been in their native state in contrast to other studies of histone chaperones, which required refolding or extracting histones from a denatured state prior to complex formation (*31*, *48*−*51*). Our coexpression approach is a valid way to make the Asf1−H3−H4 complex because it most closely approximates what would occur in the cell, i.e., cotranslational complex formation. Because the production of soluble recombinant histones in *E. coli* had never been achieved before, we viewed the ability of the histones to be produced as a soluble complex with Asf1 as a significant advancement toward obtaining a physiologically relevant complex.

The stability of the Asf1−H3−H4 heterodimer complex is quite striking. The Asf1tr−H3−H4 complex does not detectably dissociate into H3−H4 tetramers over several days at 4 °C, as measured by analytical ultracentrifugation and gel filtration analyses (Figure 6 and data not shown). Assuming that the H3−H4 tetramer would be more thermodynamically stable than the Asf1−H3−H4 complex, failure of the Asf1−H3−H4 complex to dissociate into H3−H4 tetramers indicates that there must be a kinetic barrier to the dissociation of the Asf1−H3−H4 complex. The formation of a kinetic trap for the H3−H4 dimer by Asf1 could be an important component of its function as a chaperone, as has been demonstrated recently for the pilus chaperones from *E. coli* (*52*). Asf1 would have to capture the H3−H4 dimer in the cytoplasm, preventing spontaneous assembly of the H3−H4 tetramer. Asf1 would then maintain the histones as a heterodimer, the physiological form of free histones in the cell (*31*), until they are in the vicinity of DNA. The high charge difference between the basic H3−H4 dimer and the acidic Asf1 protein may contribute to the kinetic barrier to histone dissociation, as much energy would need to be added to pull highly charged particles apart.

Asf1 must block the H3−H3 dimerization interface of the H3−H4 heterodimer, preventing formation of the H3−H4 heterotetramer and allowing soluble histones to exist as H3−H4 heterodimers. Consistent with this, there is functional evidence to indicate that the manner in which Asf1 presents histones is important for chromatin assembly. Asf1 cannot deposit purified H3−H4 heterotetramers or the histones from the 293 chromatin assembly extract onto DNA, but instead, it can only promote the assembly of chromatin from histones prebound to Asf1 [Figure 3 (*23*)]. We propose that in the cell, histone chaperones such as Asf1 bind to H3−H4 heterodimers cotranslationally and maintain the newly synthesized histones as H3−H4 heterodimers. This will in turn delay formation of the H3−H4 heterotetramer until the histones are in the vicinity of the DNA, which may serve as a trigger for their release. Consistent with this idea, Asf1 expression peaks in late G1-phase of the cell cycle immediately before histone synthesis (*12*). Furthermore, Asf1 is primarily nuclear-localized during the S-phase but not at other times of the cell cycle (*29*). The cell presumably has a mechanism to release Asf1 from H3−H4 heterodimers at the appropriate time and place, allowing the H3 dimerization interface to be exposed. This may be necessary to allow for the ordered and energetically favorable formation of the H3−H4 heterotetramer on DNA.

The fact that newly synthesized histones H3 and H4 in the presence of chaperones exist as heterodimers indicates that the mechanism of chromatin assembly must now be re-evaluated. We can confidently describe the formation of an H3−H4 heterotetramer on DNA as the simultaneous or

sequential deposition of two H3−H4 heterodimers onto DNA (Figure 7). Following DNA replication, the newly synthesized H3−H4 heterodimers do not intermingle with old H3−H4 heterodimers from the parental chromatin strand (*6*). This may reflect an active process whereby the machinery, including Asf1 and another histone chaperone termed CAF-1, deposits two newly synthesized H3−H4 heterodimers at a time onto newly replicated DNA (Figure 7). Alternatively, the failure of old and new H3−H4 heterodimers to intermingle during DNA replication may be the passive consequence of old heterotetramers remaining intact during DNA replication. This is clearly not always the case in the cell, because intermixing of new and old H3−H4 heterodimers on DNA occurs during histone exchange that is independent of DNA replication and transcription (*6*). We have previously found that Asf1 is required not only for the assembly of chromatin but also for the disassembly of chromatin (*18*, *21*). The observation that Asf1 binds to an H3−H4 heterodimer indicates that disassembly of the nucleosome is likely to involve the separation of the H3−H4 heterotetramer into two H3−H4 heterodimers bound to Asf1. As such, this work indicates that we have to consider an extra dynamic and regulated step in all processes that require chromatin assembly and disassembly, that is, the disassembly of the H3−H4 heterotetramer into H3−H4 heterodimers and the assembly of H3−H4 heterodimers into H3−H4 heterotetramers.

ACKNOWLEDGMENT

We thank Melissa Adkins and Jeffrey Linger for critical reading of the manuscript. We are grateful to Carlos Catalano and David Bain for assistance with analytical ultracentrifugation analysis, to Karolin Luger for histone expression vectors, and to Song Tan for the polycistronic expression vectors.

REFERENCES

1. Van Holde, K. E. (1989) *Chromatin*, Springer-Verlag, New York.
2. Kornberg, R. D. (1974) Chromatin structure: A repeating unit of histones and DNA, *Science 184*, 868−71.
3. Eickbush, T. H., and Moudrianakis, E. N. (1978) The histone core complex: An octamer assembled by two sets of protein−protein interactions, *Biochemistry 17*, 4955−64.
4. Arents, G., Burlingame, R. W., Wang, B. C., Love, W. E., and Moudrianakis, E. N. (1991) The nucleosomal core histone octamer at 3.1 Å resolution: A tripartite protein assembly and a left-handed superhelix, *Proc. Natl. Acad. Sci. U.S.A. 88*, 10148−52.
5. Jackson, V., Granner, D. K., and Chalkley, R. (1975) Deposition of histones onto replicating chromosomes, *Proc. Natl. Acad. Sci. U.S.A. 72*, 4440−4.
6. Jackson, V. (1990) In vivo studies on the dynamics of histone-DNA interaction: Evidence for nucleosome dissolution during replication and transcription and a low level of dissolution independent of both, *Biochemistry 29*, 719−31.
7. Annunziato, A. T. (2005) Split Decision: What Happens to Nucleosomes during DNA Replication? *J. Biol. Chem. 280*, 12065−8.
8. Tyler, J. K. (2002) Chromatin assembly. Cooperation between histone chaperones and ATP-dependent nucleosome remodeling machines, *Eur. J. Biochem. 269*, 2268−74.
9. Smith, S., and Stillman, B. (1989) Purification and characterization of CAF-I, a human cell factor required for chromatin assembly during DNA replication in vitro, *Cell 58*, 15−25.
10. Tyler, J. K., Adams, C. R., Chen, S. R., Kobayashi, R., Kamakaka, R. T., and Kadonaga, J. T. (1999) The RCAF complex mediates chromatin assembly during DNA replication and repair, *Nature 402*, 555−60.
11. Groth, A., Ray-Gallet, D., Quivy, J. P., Lukas, J., Bartek, J., and Almouzni, G. (2005) Human Asf1 Regulates the Flow of S Phase Histones during Replicational Stress, *Mol. Cell 17*, 301−11.
12. Le, S., Davis, C., Konopka, J. B., and Sternglanz, R. (1997) Two new S-phase-specific genes from *Saccharomyces cerevisiae*, *Yeast 13*, 1029−42.
13. Singer, M. S., Kahana, A., Wolf, A. J., Meisinger, L. L., Peterson, S. E., Goggin, C., Mahowald, M., and Gottschling, D. E. (1998) Identification of high-copy disruptors of telomeric silencing in *Saccharomyces cerevisiae*, *Genetics 150*, 613−32.
14. Mousson, F., Lautrette, A., Thuret, J. Y., Agez, M., Courbeyrette, R., Amigues, B., Becker, E., Neumann, J. M., Guerois, R., Mann, C., and Ochsenbein, F. (2005) Structural basis for the interaction of Asf1 with histone H3 and its functional implications, *Proc. Natl. Acad. Sci. U.S.A. 102*, 5975−80.
15. Munakata, T., Adachi, N., Yokoyama, N., Kuzuhara, T., and Horikoshi, M. (2000) A human homologue of yeast anti-silencing factor has histone chaperone activity, *Genes Cells 5*, 221−33.
16. Umehara, T., Chimura, T., Ichikawa, N., and Horikoshi, M. (2002) Polyanionic stretch-deleted histone chaperone cia1/Asf1p is functional both in vivo and in vitro, *Genes Cells 7*, 59−73.
17. Daganzo, S. M., Erzberger, J. P., Lam, W. M., Skordalakes, E., Zhang, R., Franco, A. A., Brill, S. J., Adams, P. D., Berger, J. M., and Kaufman, P. D. (2003) Structure and function of the conserved core of histone deposition protein Asf1, *Curr. Biol. 13*, 2148−58.
18. Adkins, M. W., and Tyler, J. K. (2004) The histone chaperone Asf1p mediates global chromatin disassembly in vivo, *J. Biol. Chem. 279*, 52069−74.
19. Sutton, A., Bucaria, J., Osley, M. A., and Sternglanz, R. (2001) Yeast asf1 protein is required for cell cycle regulation of histone gene transcription, *Genetics 158*, 587−96.
20. Chimura, T., Kuzuhara, T., and Horikoshi, M. (2002) Identification and characterization of CIA/ASF1 as an interactor of bromodomains associated with TFIID, *Proc. Natl. Acad. Sci. U.S.A. 99*, 9334−9.
21. Adkins, M. W., Howar, S. R., and Tyler, J. K. (2004) Chromatin disassembly mediated by the histone chaperone Asf1 is essential for transcriptional activation of the yeast PHO5 and PHO8 genes, *Mol. Cell 14*, 657−66.
22. Zabaronick, S. R., and Tyler, J. K. (2005) The histone chaperone anti-silencing function 1 is a global regulator of transcription independent of passage through S phase, *Mol. Cell. Biol. 25*, 652−60.
23. Sharp, J. A., Fouts, E. T., Krawitz, D. C., and Kaufman, P. D. (2001) Yeast histone deposition protein Asf1p requires Hir proteins and PCNA for heterochromatic silencing, *Curr. Biol. 11*, 463−73.
24. Meijsing, S. H., and Ehrenhofer-Murray, A. E. (2001) The silencing complex SAS-I links histone acetylation to the assembly of repressed chromatin by CAF-I and Asf1 in *Saccharomyces cerevisiae*, *Genes Dev. 15*, 3169−82.
25. Osada, S., Sutton, A., Muster, N., Brown, C. E., Yates, J. R., III, Sternglanz, R., and Workman, J. L. (2001) The yeast SAS (something about silencing) protein complex contains a MYST-type putative acetyltransferase and functions with chromatin assembly factor ASF1, *Genes Dev. 15*, 3155−68.
26. Myung, K., Smith, S., and Kolodner, R. D. (2004) Mitotic checkpoint function in the formation of gross chromosomal rearrangements in *Saccharomyces cerevisiae*, *Proc. Natl. Acad. Sci. U.S.A. 101*, 15980−5.
27. Prado, F., Cortes-Ledesma, F., and Aguilera, A. (2004) The absence of the yeast chromatin assembly factor Asf1 increases genomic instability and sister chromatid exchange, *EMBO Rep. 5*, 497−502.
28. Ramey, C. J., Howar, S., Adkins, M., Linger, J., Spicer, J., and Tyler, J. K. (2004) Activation of the DNA damage checkpoint in yeast lacking the histone chaperone anti-silencing function 1, *Mol. Cell. Biol. 24*, 10313−27.
29. Moshkin, Y. M., Armstrong, J. A., Maeda, R. K., Tamkun, J. W., Verrijzer, P., Kennison, J. A., and Karch, F. (2002) Histone chaperone ASF1 cooperates with the Brahma chromatin-remodelling machinery, *Genes Dev. 16*, 2621−6.
30. Wolffe, A. P. (1998) *Chromatin structure and function*, 3rd ed., Academic Press, San Diego.
31. Tagami, H., Ray-Gallet, D., Almouzni, G., and Nakatani, Y. (2004) Histone H3.1 and H3.3 complexes mediate nucleosome assembly pathways dependent or independent of DNA synthesis, *Cell 116*, 51−61.

32. Tan, S. (2001) A modular polycistronic expression system for overexpressing protein complexes in *Escherichia coli*, *Protein Expression Purif. 21*, 224−34.
33. Stafford, W. F., III (1992) Boundary analysis in sedimentation transport experiments: A procedure for obtaining sedimentation coefficient distributions using the time derivative of the concentration profile, *Anal. Biochem. 203*, 295−301.
34. Philo, J. S. (2000) A method for directly fitting the time derivative of sedimentation velocity data and an alternative algorithm for calculating sedimentation coefficient distribution functions, *Anal. Biochem. 279*, 151−63.
35. Stafford, W. F. (1997) Sedimentation velocity spins a new weave for an old fabric, *Curr. Opin. Biotechnol. 8*, 14−24.
36. Laue, T. M. (1995) Sedimentation equilibrium as thermodynamic tool, *Methods Enzymol. 259*, 427−52.
37. Luger, K., Mader, A. W., Richmond, R. K., Sargent, D. F., and Richmond, T. J. (1997) Crystal structure of the nucleosome core particle at 2.8 Å resolution, *Nature 389*, 251−60.
38. Baxevanis, A. D., Godfrey, J. E., and Moudrianakis, E. N. (1991) Associative behavior of the histone $(H3-H4)_2$ tetramer: Dependence on ionic environment, *Biochemistry 30*, 8817−23.
39. Wang, J. C. (1982) The path of DNA in the nucleosome, *Cell 29*, 724−6.
40. Philo, J. S., Yang, T. H., and LaBarre, M. (2004) Re-examining the oligomerization state of macrophage migration inhibitory factor (MIF) in solution, *Biophys. Chem. 108*, 77−87.
41. Durchschlag, H. (1986) Specific volumes of biological macromolecules and some other molecules of biological interest, in *Thermodynamic Data for Biochemistry and Biotechnology*, pp 45−128, Springer-Verlag, Berlin.
42. Akey, C. W., and Luger, K. (2003) Histone chaperones and nucleosome assembly, *Curr. Opin. Struct. Biol. 13*, 6−14.
43. Dutnall, R. N. (2004) Nucleosome assembly: More than electric in the making? *Structure 12*, 2098−100.
44. Kornberg, R. D., and Thomas, J. O. (1974) Chromatin structure; oligomers of the histones, *Science 184*, 865−8.
45. Roark, D. E., Geoghegan, T. E., and Keller, G. H. (1974) A two-subunit histone complex from calf thymus, *Biochem. Biophys. Res. Commun. 59*, 542−7.
46. D'Anna, J. A., Jr., and Isenberg, I. (1974) A histone cross-complexing pattern, *Biochemistry 13*, 4992−7.
47. Smith, P. A., Jackson, V., and Chalkley, R. (1984) Two-stage maturation process for newly replicated chromatin, *Biochemistry 23*, 1576−81.
48. Loyola, A. L. G., Wang, Y.-H., and Reinberg, D. (2001) Reconstitution of recombinant chromatin establishes a requirement for histone-tail modifications during chromatin assembly and transcription, *Genes Dev. 15*, 2837−51.
49. Levenstein, M. E., and Kadonaga, J. T. (2002) Biochemical analysis of chromatin containing recombinant *Drosophila* core histones, *J. Biol. Chem. 277*, 8749−54.
50. Fejes Toth, K., Mazurkiewicz, J., and Rippe, K. (2005) Association states of nucleosome assembly protein 1 and its complexes with histones, *J. Biol. Chem. 280*, 15690−9.
51. Park, Y. J., Chodaparambil, J. V., Bao, Y., McBryant, S. J., and Luger, K. (2005) Nucleosome assembly protein 1 exchanges histone H2A−H2B dimers and assists nucleosome sliding, *J. Biol. Chem. 280*, 1817−25.
52. Vetsch, M., Puorger, C., Spirig, T., Grauschopf, U., Weber-Ban, E. U., and Glockshuber, R. (2004) Pilus chaperones represent a new type of protein-folding catalyst, *Nature 431*, 329−33.

BI051333H